

On corrosion-induced cracking in reinforced concrete with different corrosion rates

Ismail Aldellaa*, Peter Grassl

James Watt School of Engineering, University of Glasgow, Glasgow, UK
i.aldellaa.1@research.gla.ac.uk, peter.grassl@glasgow.ac.uk

Abstract

Corrosion of steel in structural concrete occurs naturally at low corrosion rates, so that corrosion products accumulate over years adjacent to the steel surface before sufficient pressure is generated to induce cracks in the concrete cover [3]. In research studies, the corrosion process is accelerated by impressing currents to obtain cracking of the concrete cover in a few days [11]. For being able to predict corrosion induced cracking, it is required to link the accelerated process to naturally occurring corrosion. The aim of this paper is to evaluate the capabilities modelling approaches to predict the effect of corrosion rates by comparing the models with experiments carried out within this study. In the experiments, accelerated corrosion tests are carried out by applying three different corrosion rates on thick-walled cylinders with a single reinforcement bar in the centre. Four different concrete mixes are used. For the modelling, a lattice model based on a three-dimensional discretisation of the thick-walled cylinder and an inelastic axis-symmetric thick-walled cylinder model with advancing crack front are used. The lattice model is implemented in the finite element program OOFEM [10]. In the models, the basic creep is predicted with the B3 model described in Bažant and Baweja [2].

Key words: *Concrete; Corrosion; Cracking; Lattice modelling*

1 Introduction

Corrosion induced cracking is considered as the main deterioration mechanism which affects the service life of reinforced concrete structures [3]. The process of corrosion of reinforcement in concrete structures is divided into an initiation and propagation period. The first stage describes the ingress of chloride or carbon dioxide into the concrete cover to reach the rebar which leads to the loss of the passive layer adjacent to the surface of the reinforcing steel. Then, in the propagation stage, the corrosion process of steel starts. Once corrosion is initiated, corrosion products (rust) accumulate near the concrete-rebar interface. Since the corrosion products have a lower density than steel, their formation generates radial pressure on the concrete cover, which causes eventually surface cracking and spalling [12]. To be able to predict the deterioration due to corrosion so that structures can be repaired cost-effectively, it is important to develop models which predict the corrosion-induced cracking process.

The natural corrosion rate of steel within reinforced concrete structures is very small, which leads to corrosion products accumulating for years before causing a visible crack [3]. Therefore, in research laboratories, corrosion is usually accelerated by impressing a current on the rebar to gain the required damage in the concrete cover within days [11]. It is commonly assumed that the results of these accelerated tests cannot be immediately extrapolated to applications with natural corrosion rates, because corrosion rate affects factors such as migration of corrosion products into voids and cracks, as well as the composition of the products themselves [11]. The paper aims to evaluate the capabilities of modelling approaches to predict the effect of corrosion rates by comparing the models with experiments carried out within this study.

2 Methodology

An experimental setup was developed to test corrosion induced cracking at different corrosion rates. Furthermore, two mathematical modelling approaches were used to evaluate the capabilities of modelling approaches to predict the effect of corrosion rates on corrosion induced cracking. The experimental setup and models are described in the following sections.

2.1 Experiment

Concrete cylinders with a single steel rebar in the centre were used for accelerated corrosion tests. The cylinders were made by using four concrete mixes with different w/c ratios. The ratios are 0.38, 0.45, 0.55 and 0.70, which resulted in compressive strengths of 53, 37, 29 and 18 MPa respectively. The geometry of test specimens has a diameter of 150 mm and a height of 100 mm. The reinforcement has a diameter of 16 mm. The geometry of the thick-walled cylinder that is used in the experiments is shown in Figure 1b. For accelerating corrosion, 2 percent sodium chloride (w/w) was added to the cement in order to initiate corrosion. During the test, the cylinders were immersed in tanks with 5 percent (w/w) sodium chloride solution [5, 4]. To speed up the corrosion process, three different corrosion rates were applied which were approximately ($50 \mu\text{A}/\text{cm}^2$, $100 \mu\text{A}/\text{cm}^2$ and $500 \mu\text{A}/\text{cm}^2$) [11]. The setup of the accelerated corrosion test consists of applying a constant current from a DC power supply to the steel rebar embedded in the specimen, which is immersed in tanks with chloride solution with the copper mesh to let the electrons travel between the rebar and copper, which act as anode and cathode, respectively. For identifying the first surface crack at the beginning of the corrosion process and to measure the crack width, two methods were used, namely application of strain gauges around the circumference of the cylinder and digital crack measurement. The corrosion penetration dx_{cor} can be calculated from the determined time of cracking initiation by using the following equation for both methods:

$$dx_{\text{cor}} = 0.0315i_{\text{cor}}dt \quad (1)$$

where dx_{cor} in μm , i_{cor} is the corrosion rate in $\mu\text{A}/\text{cm}^2$, dt is time in days, and 0.0315 is a factor to convert $\mu\text{m}/\text{day}$ into $\mu\text{A}/\text{cm}^2$ as stated in Molina et al. [9].

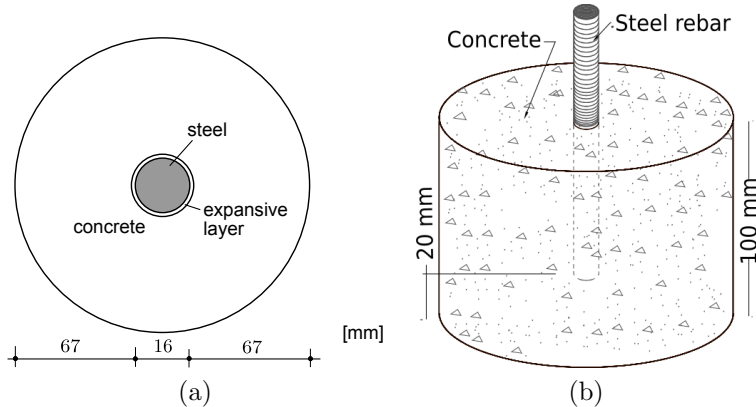


Figure 1: (a) Geometry of the thick-walled cylinder for experiments and models. The out-of-plane thickness for models is 10 mm. (b) Geometry of specimen in experiments.

2.2 Modelling

Two numerical models are evaluated for predicting the effect of corrosion rates on surface cracking. These two models were compared with experiments performed in this study. The first approach is based on a cracked axis-symmetric thick-walled cylinder. In this model, the cylinder is subdivided into two parts, namely cracked and uncracked cylinders. The inner pressure is controlled by increasing the radius of the cracked cylinder incrementally [1, 7]. In this model, cracking is considered by smearing out the crack opening over the circumference of the cylinder. The crack is initiated once the circumferential stress reaches the tensile strength. The second approach is a lattice model, which is based on a three-dimensional discretisation of the thick-walled cylinder presented earlier in Grassl and Davies [6], which was implemented in the finite element program OOFEM (<http://www.oofem.org>). The mesostructure of concrete was represented by using autocorrelated

random fields for both tensile and compressive strengths. To implement creep in OOFEM, the microstress-solidification theory (MPS) was used [8]. To model the age-dependence of tensile strength, the fib Model Code 2010 was used. The two models are described in detail in [1]. The corrosion penetration dx_{cor} is calculated from the determined time of crack initiation by using the equation mentioned above for both models. The expansion factor of $\alpha = 2$ is used in the analysis as in most of the previous studies. For the axisymmetric model, the cylinder cracks as a result of the critical inner radial displacement (which is equal to the critical corrosion penetration). The lattice model provides information about crack patterns and force distributions at each stage of analysis in detail. The geometry of the thick-walled cylinder for both models has the same diameter as the concrete cylinder used in the experiments as shown in Figure 1a. However, for the thick-walled cylinder model, plane stress conditions are applied. For the lattice approach, a thin slice of 10 mm is modelled. For both models, first the parameters were calibrated to obtain the value of tensile strength f_t and Young's modulus E for the test specimens for short term loading at 28 days, which are $f_t = 3.35$ MPa and $E = 33.3$ GPa.

3 Results

Both in the experiments and models, three corrosion rates of $i_{\text{cor}} = 50, 100$ and $500 \mu\text{A}/\text{cm}^2$ were used to determine the amount of corrosion penetration at which the surface crack is initiated. The corrosion process was initiated at a concrete age of 535 days. The time of the initiation of surface cracking was used to obtain the critical corrosion penetration from equation 1 for the experiments and models. From Figure 2a the accelerated corrosion test results shows that the critical corrosion penetration is not strongly influenced by the corrosion rates used in this study. The modelling results show that there is no visible effect of the different corrosion rates on the critical corrosion penetration. The crack patterns after surface cracking for both lattice model and experiment shown in Figure 2b agree well.

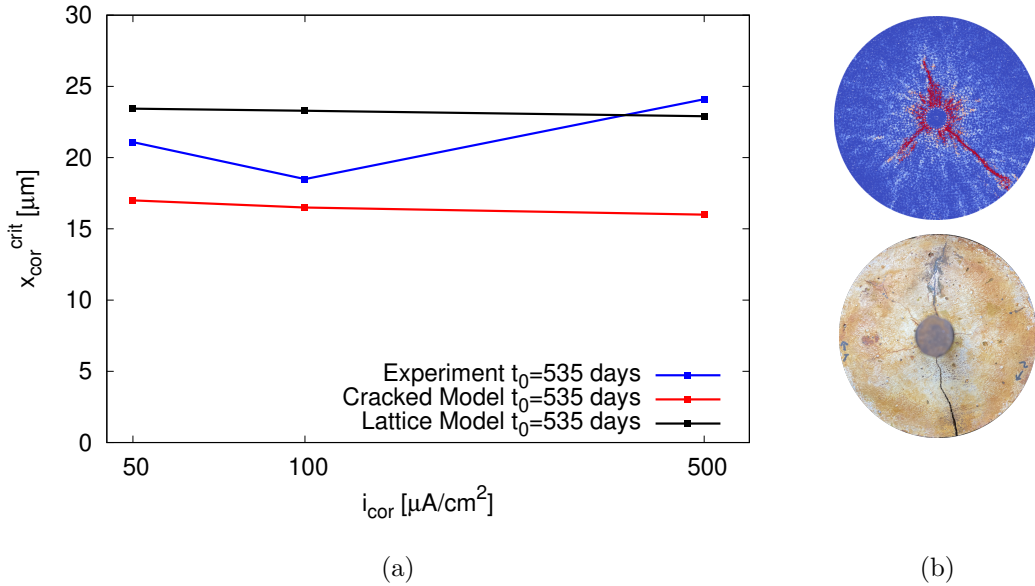


Figure 2: Results of analyses and experiments: (a) Critical corrosion penetration versus corrosion rate for experiment and two models. (b) The crack patterns after concrete cover cracked from lattice model for $i_{\text{cor}} = 500 \mu\text{A}/\text{cm}^2$ with an equivalent crack width $\bar{w}_c > 2 \mu\text{m}$ and experiment at crack width $\bar{w}_c > 1.5\text{mm}$.

4 Conclusions

The results of this study shown that for the corrosion test used here, the effect of corrosion rate on the critical corrosion penetration is not clearly visible from the experiments. Furthermore, for both modelling approaches, no effect of corrosion rates on critical corrosion penetration was visible. However, the results show that the critical corrosion penetration depends on the modelling type. The lattice model results in higher critical corrosion penetration than cracked model, which, for two of the three corrosion rates, is closer to the experimental results.

Acknowledgments

Ismail Adellaa acknowledges the financial support from the Ministry of Higher Education - Libya. The lattice simulations were performed with the finite element program OOFEM [10].

References

- [1] Aldellaa, I.; Havlásek, P.; Jirásek, M., and Grassl, P. Effect of creep on corrosion-induced cracking. *Engineering Fracture Mechanics*, page 108310, 2022.
- [2] Bažant, Z. P. and Baweja, S. Creep and shrinkage prediction model for analysis and design of concrete structures – model B3. *Materials and Structures*, 28:357–365, 1995. RILEM Recommendation, in collaboration with RILEM Committee TC 107-GCS, with Errata, Vol. 29 (March 1996), p. 126.
- [3] Broomfield, J. P. *Corrosion of steel in concrete: understanding, investigation and repair*. Taylor & Francis, 1997.
- [4] Cairns, J.; Du, Y., and Law, D. Structural performance of corrosion-damaged concrete beams. *Magazine of Concrete Research*, 60(5):359–370, 2008.
- [5] El Maaddawy, T. and Soudki, K. A. Effectiveness of impressed current technique to simulate corrosion of steel reinforcement in concrete. *Journal of materials in civil engineering*, 15(1): 41–47, 2003.
- [6] Grassl, P. and Davies, T. Lattice modelling of corrosion induced cracking and bond in reinforced concrete. *Cement and Concrete Composites*, 33:918–924, 2011.
- [7] Grassl, P.; Jirásek, M., and Gallipoli, D. Initiation of fluid-induced fracture in a thick-walled hollow permeable sphere. *European Journal of Mechanics-A/Solids*, 76:123–134, 2019.
- [8] Jirásek, M. and Havlásek, P. Accurate approximations of concrete creep compliance functions based on continuous retardation spectra. *Computers and Structures*, 135:155–168, 2014.
- [9] Molina, F.; Alonso, C., and Andrade, C. Cover cracking as a function of rebar corrosion: Part II-numerical model. *Materials and Structures*, 26(9):532–548, 1993.
- [10] Patzák, B. OOFEM – An object-oriented simulation tool for advanced modeling of materials and structure. *Acta Polytechnica*, 52:59–66, 2012.
- [11] Pedrosa, F. and Andrade, C. Corrosion induced cracking: Effect of different corrosion rates on crack width evolution. *Construction and Building Materials*, 133:525–533, 2017.
- [12] Tuutti, K. Corrosion of steel in concrete. Doctoral thesis, Swedish Cement and Concrete Research Institute, 1982.